Proc. Natl. Acad. Sci. USA
Vol. 94, pp. 8450–8455, August 1997
Biochemistry

Structural flexibility in transcription complex formation revealed by protein–DNA photocrosslinking

MICHELE A. CLEARY*†, P. SHANNON PENDERGRAST*‡, AND WINSHIP HERR*§

*Cold Spring Harbor Laboratory, Cold Spring Harbor, NY 11724; and ‡Howard Hughes Medical Institute, Cold Spring Harbor Laboratory, Cold Spring Harbor, NY 11724

Communicated by James D. Watson, Cold Spring Harbor Laboratory, Long Island, NY, May 29, 1997 (received for review April 4, 1997)

ABSTRACT The Oct-1 POU domain binds diverse DNA-sequence elements and forms a higher-order regulatory complex with the herpes simplex virus coregulator VP16. The POU domain contains two separate DNA-binding domains joined by a flexible linker. By protein–DNA photocrosslinking we show that the relative positioning of the two POU DNA-binding domains on DNA varies depending on the nature of the DNA target. On a single VP16-responsive element, the POU domain adopts multiple conformations. To determine the structure of the Oct-1 POU domain in a multiprotein complex with VP16, we allowed VP16 to interact with previously crosslinked POU-domain–DNA complexes and found that VP16 can associate with multiple POU-domain conformations. These results reveal the dynamic potential of a DNA-binding domain in directing transcriptional regulatory complex formation.

The human transcriptional activator protein Oct-1, which contains a DNA-binding POU domain, displays diversity in DNA-sequence recognition and coregulator association. The POU domain is a bipartite DNA-binding structure made up of two helix–turn–helix-containing DNA-binding domains: a POU-specific (POU$_S$) domain joined by a flexible linker to a carboxy-terminal POU-homeo (POU$_H$) domain (1–3). The Oct-1 POU domain displays exceptional sequence recognition flexibility and directs complex formation with viral and cellular coregulators, including the herpes simplex virus transactivator VP16 (Vmw65, αTIF) (reviewed in ref. 4).

DNA-binding studies of POU domains have revealed a high degree of structural flexibility in their interactions with DNA. For example, the x-ray crystal structures of the Oct-1 and Pit-1 POU domains bound to Oct-1- and Pit-1-responsive sites, respectively, differ: The Oct-1 POU domain binds to the octamer sequence ATGCAAAT as a monomer, with the POU$_S$ and POU$_H$ domains bound to opposite faces of the DNA (2), whereas the Pit-1 POU domain binds its site as a dimer with the POU$_S$ and POU$_H$ domains of each POU domain bound to the same face of the DNA and with the POU$_S$ domain in an inverted orientation to that found with Oct-1 (3). Furthermore, combined mutagenesis of the Oct-1 or related Brn-2 POU domains and their respective DNA targets has provided indirect evidence that even the same POU domain adopts different conformations on different cis-regulatory sites, providing a mechanism for divergent sequence recognition (5, 6).

To probe directly the conformational flexibility of the Oct-1 POU domain bound to DNA and in a higher-order complex, we adapted a site-specific protein–DNA photocrosslinking protocol (7) to map, individually, the locations of the POU$_S$ and POU$_H$ domains on DNA and in complex with VP16. Our results show that the Oct-1 POU domain adopts multiple conformations on a single binding site and in association with VP16.

MATERIALS AND METHODS

***In Vitro* Mutagenesis.** The site-specific protein–DNA photocrosslinking method we used (7) involves the attachment of the photoactivatable crosslinker 4-azidophenacyl bromide to an appropriately positioned unique cysteine in the DNA-binding protein. We removed the existing Oct-1 POU domain cysteines at positions 61 of the POU$_S$ domain and 50 of the POU$_H$ domain and introduced unique cysteines by oligonucleotide-mediated site-directed mutagenesis (6). To create unique cysteine (UC) derivatives, we made the following POU$_S$ mutations: L23C (POU$_{S\text{-}UC23}$), G24C (POU$_{S\text{-}UC24}$), F25C (POU$_{S\text{-}UC25}$), G28C (POU$_{S\text{-}UC28}$), D29C (POU$_{S\text{-}UC29}$), and N54C (POU$_{S\text{-}UC54}$); and the following POU$_H$ mutations: S7C (POU$_{H\text{-}UC7}$), E9C (POU$_{H\text{-}UC9}$), and T10C (POU$_{H\text{-}UC10}$).

4-Azidophenacyl-Bromide Modification. Oct-1 POU-domain variants were prepared in *Escherichia coli* as glutathione *S*-transferase (GST)-fusion proteins essentially as described (8). Purified POU domain was cleaved from the GST moiety (3.5 μM in 500 μl) with thrombin and treated for 6 hr at room temperature in the dark with 140 μM 4-azidophenacyl bromide (Sigma) and 1.7% dimethylformamide as described (7). Reaction mixtures were then dialyzed twice against 1 liter of 20 mM Tris·HCl, pH 8.0/200 mM KCl/5% glycerol/0.1 mM EDTA for a total of 14 hr.

POU Domain–DNA Photocrosslinking and Site-Specific Cleavage. POU domain–DNA binding reactions (100 μl in flat-bottomed microtiter plate wells) contained 0.28 μM Oct-1 POU domain protein, 3 × 10^5 cpm of the appropriate singly end-labeled DNA probe generated by PCR amplification (see ref. 6) in 8 mM Na·Hepes, pH 7.9/60 mM NaCl/4 mM spermidine/2 mM EDTA/0.2 mM DTT/0.03% Nonidet P-40/0.1 mg/ml bovine serum albumin. Reaction mixtures were incubated at room temperature for 30 min in the dark before being irradiated for 1.5 min in a UV Stratalinker 2400 (Stratagene) with 312-nm UV bulbs. The irradiation time was determined empirically for optimal crosslinking. After UV irradiation, 5 μl of each binding reaction mix was removed, added to 5 μl of SDS loading buffer, heated to 90°C for 10 min, and subjected to 10% SDS/PAGE in the absence of a stacking gel. Levels of crosslinking (typically 3%) were determined by phosphorimager analysis (Fuji BAS1000). The remainder of the sample was used to map the sites of crosslinking as described (7). Purine cleavage patterns for each probe were generated as described (9). DNA cleavage products were analyzed on 20% polyacrylamide/7 M urea denaturing gels.

The publication costs of this article were defrayed in part by page charge payment. This article must therefore be hereby marked "*advertisement*" in accordance with 18 U.S.C. §1734 solely to indicate this fact.

Abbreviation: UC, unique cysteine.

†Present address: Howard Hughes Medical Institute and Department of Molecular Biology, Princeton University, Princeton, NJ 08544.

§To whom reprint requests should be addressed. e-mail: herr@cshl.org.

Crosslinking Interference Analysis. POU$_{\text{S-UC54}}$ or POU$_{\text{H-UC50}}$ was allowed to bind to the (OCTA^{+})TAATGARAT probe and crosslinked to the DNA as described above except that, after UV-induced crosslinking, *E. coli*-expressed GST–VP16 and an *in vitro*-translated form of the VP16-induced complex accessory factor HCF (10) were added, and the reaction was incubated for 20 min at 37°C. The protein–DNA complexes were separated on a native 4% polyacrylamide/0.25× TBE gel, and bands corresponding to the VP16-induced and POU-domain complexes were cut out of the gel, soaked in 20 mM ammonium acetate, 0.1 mM EDTA, and 2% SDS at 4°C overnight and spun through Spin-X filters (Costar). The eluted protein/DNA was treated as described for cleavage at sites of crosslinking (7), and the cleavage products were mapped by denaturing PAGE.

RESULTS

Experimental Design. Pendergrast *et al.* (7) have described a site-specific protein–DNA photocrosslinking method in which the photoactivatable crosslinking agent 4-azidophenacyl bromide is covalently attached to a unique cysteine side chain on the surface of a DNA-binding protein. The modified protein is allowed to bind to DNA, and the binding reaction is then subjected to UV irradiation, enabling the modified cysteine side chain to form a covalent bond with nearby DNA. Crosslinked protein–DNA complexes are then analyzed directly by SDS/PAGE or the sites of crosslinking mapped by site-specific crosslink-induced DNA cleavage (7). We created Oct-1 POU domains carrying either POU$_{\text{S}}$- or POU$_{\text{H}}$-domain-specific crosslinkers. These domain-specific crosslinkers allowed us to probe independently the positions of the two Oct-1 POU DNA-binding domains on cis-regulatory sites.

We examined Oct-1 POU-domain binding to three previously described sites (see ref. 6): the high-affinity octamer sequence ATGCAAAT from the human histone H2B promoter [for which the structure of the bound Oct-1 POU domain is known (2)] and two VP16-responsive TAATGARAT (R = purine) elements derived from the herpes simplex virus ICP0 [called (OCTA^{+})TAATGARAT] and ICP4 [called (OCTA^{-})TAATGARAT] immediate-early (IE) promoters. These two sites represent the two different kinds of TAATGARAT elements found in herpes simplex virus IE promoters (see ref. 11); only (OCTA^{+})TAATGARAT elements contain an overlapping octamer sequence (shown in bold: **ATGCTAAT**GARAT).

Fig. 1*A* shows a representation of the crystal structure of the Oct-1 POU domain bound to the histone H2B octamer site (2), with the POU$_{\text{S}}$ domain considered 5′ of the POU$_{\text{H}}$ domain. The structure of the Oct-1 POU domain on a TAATGARAT site is not known. Mutational analysis has suggested that on an (OCTA^{-})TAATGARAT site, the POU$_{\text{S}}$ domain lies 3′ of the POU$_{\text{H}}$ domain (6), and high-resolution hydroxy-radical footprinting of an Oct-1 POU domain–(OCTA^{+})TAATGARAT complex revealed only protection of the TAAT sequence, suggesting an unusual POU-domain conformation on this site (12).

To generate Oct-1 POU domains with unique cysteines suitable for protein–DNA crosslinking, we created the cysteine-free double mutant POU$_{\text{S-C61A}}$/POU$_{\text{H-C50S}}$ by replacing the wild-type POU$_{\text{S}}$-domain cysteine with an alanine and the wild-type POU$_{\text{H}}$-domain cysteine with a serine. This cysteine-free Oct-1 POU domain binds like wild-type POU domain to the octamer, and (OCTA^{+}) and (OCTA^{-}) TAATGARAT sites (13). Directed by the structure of the Oct-1 POU domain–octamer site complex (2), we placed unique cysteines at a number of POU$_{\text{S}}$- and POU$_{\text{H}}$-domain positions that (*i*) were likely not to be important for DNA binding and (*ii*) whose α carbons were ≈9–13 Å from the DNA. The ability of these mutant proteins to crosslink to DNA was analyzed by SDS/PAGE. Of six POU$_{\text{S}}$-domain derivatives tested (see *Materials and Methods*), only POU$_{\text{S-UC54}}$ crosslinked to the octamer or (OCTA^{-})TAATGARAT sites effectively, and, of the four POU$_{\text{H}}$-domain derivatives tested (see *Materials and Methods*), only POU$_{\text{H-UC7}}$ and POU$_{\text{H-UC50}}$ crosslinked effectively (data not shown).

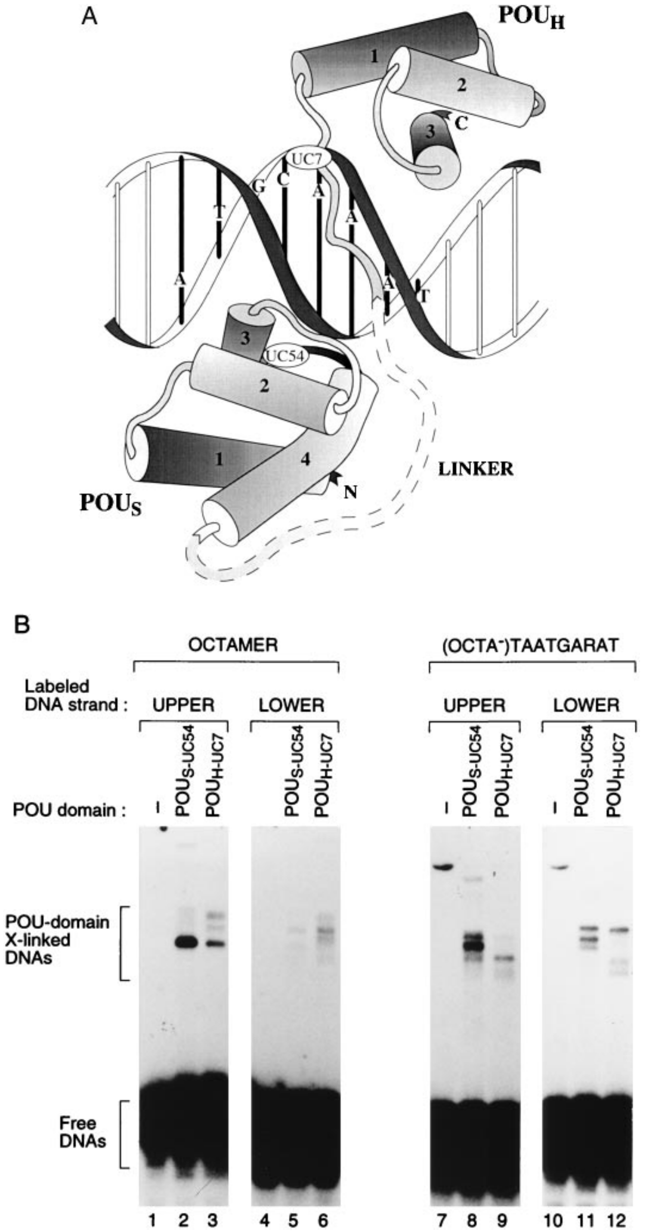

FIG. 1. Unique cysteines in the POU$_{\text{S}}$ and POU$_{\text{H}}$ domains effective for protein–DNA crosslinking. (*A*) Representation (adapted from refs. 2 and 4) of the Oct-1 POU domain–octamer site crystal structure with the positions of the unique cysteines used for crosslinking analysis indicated (UC54 in the POU$_{\text{S}}$ domain and UC7 in the POU$_{\text{H}}$ domain; the precise location of UC54 is hidden behind helix 2 on the turn between helices 3 and 4). (*B*) SDS/PAGE analysis of crosslinked protein–DNA complexes after UV irradiation of POU domain-binding reactions containing no protein (lanes 1, 4, 7, and 10), POU$_{\text{S-UC54}}$ protein (lanes 2, 5, 8, and 11), or POU$_{\text{H-UC7}}$ protein (lanes 3, 6, 9, and 12). Shown are crosslinked complexes formed on the upper and lower strands of the histone H2B octamer and the (OCTA^{-})TAATGARAT sites, as indicated.

Fig. 1*B* shows the results of crosslinking POU$_{\text{S-UC54}}$ and POU$_{\text{H-UC7}}$ to the octamer and the (OCTA^{-})TAATGARAT sites as analyzed by SDS/PAGE in the absence of a stacking gel. The slower migrating complexes probably represent POU-domain crosslinked DNAs because formation of these species depended on (*i*) added POU domain (Fig. 1*B*; a nonspecific slower migrating species in lanes 7 and 10 formed in the absence of POU domain), (*ii*) UV irradiation, (*iii*) modification of the protein with 4-azidophenacyl bromide, and (*iv*) an appropriately positioned cysteine (data not shown). Some crosslinked samples produced more than one band (lanes 3, 6, 8, 9, 11, and 12), which may reflect POU-domain crosslinking at different positions in the DNA.

The Oct-1 POU Domain Adopts Different Conformations on the Octamer and (OCTA$^-$)TAATGARAT Sites. Although both strands of the octamer and (OCTA$^-$)TAATGARAT sites could be crosslinked to the POU domain (Fig. 1*B*), only the upper strands of these probes were good substrates for site-specific DNA cleavage (data not shown). Fig. 2 shows the cleavage patterns that map sites of POU$_S$- and POU$_H$-domain crosslinking to the upper strands of these two sites. On the upper strand of the octamer probe, the primary site of crosslink-induced cleavage by the modified POU$_{S\text{-}UC54}$ protein (lane 2) maps to the G at the third position of the octamer sequence (AT<u>G</u>CAAAT) and is consistent with the POU domain–octamer site crystal structure (2). The POU$_{H\text{-}UC7}$ protein generated two cleavage products (Fig. 2, lane 3). These products map to the G and C at positions 3 and 4 (AT<u>GC</u>AAAT) and are also consistent with the POU domain–octamer site crystal structure (2).

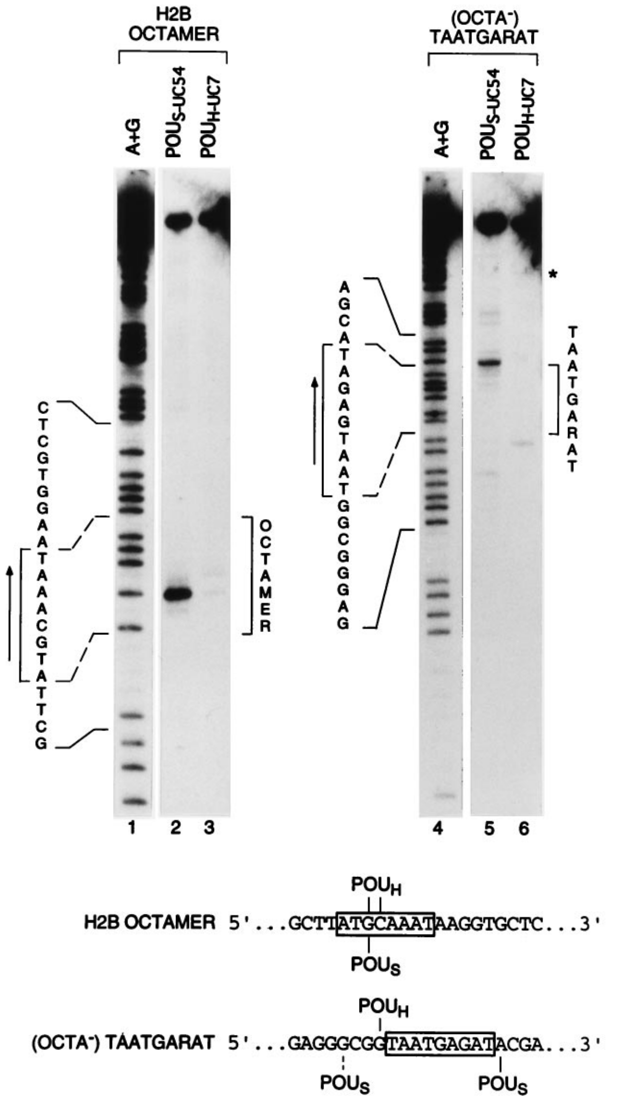

FIG. 2. The POU$_S$ domain is located on opposite sides of the POU$_H$ domain on octamer and (OCTA$^-$)TAATGARAT sites. Shown are the cleavage products generated after crosslinking of POU$_{S\text{-}UC54}$ and POU$_{H\text{-}UC7}$ proteins to the upper strands of the octamer (lanes 2 and 3) and the (OCTA$^-$)TAATGARAT (lanes 5 and 6) sites, as indicated. Lanes 1 and 4 (A+G), purine-cleavage pattern of the probe indicated. In lanes 2, 3, 5, and 6, uppermost bands represent uncleaved DNA. Brackets mark the limits of the two sequences on the autoradiographs, and arrows indicate the directionality of each consensus motif. The two binding sites are cloned into the same plasmid in opposite orientations. *, Cleavage product mapping to flanking polylinker sequence, probably resulting from non-octamer-site binding. (*Lower*) Summary of positions of crosslink-induced cleavage. Dashed line indicates lower-yield cleavage product.

On the (OCTA$^-$)TAATGARAT site (Fig. 2, lanes 4–6), the primary POU$_{H\text{-}UC7}$ protein crosslink-induced cleavage (lane 6) maps to the G just 5′ of the TAATGARAT sequence (<u>G</u>TAATGAGAT). The location of this crosslink suggests that the TAAT sequence serves as the POU$_H$ domain-binding site the same way the AAAT sequence does in the octamer sequence. In contrast, the major POU$_{S\text{-}UC54}$ cleavage product maps to the opposite side of the TAAT POU$_H$ domain-binding site, at an A immediately 3′ of the GARAT sequence (TAATGAGAT<u>A</u>). Together with the POU$_H$-domain cleavage product, this predominant POU$_S$-domain cleavage product provides physical evidence that the POU domain can adopt a conformation on an (OCTA$^-$)TAATGARAT sequence that is very different from its conformation on an octamer sequence.

In addition to the major 3′ POU$_S$-domain cleavage product, there are several minor cleavage products including one resulting from a crosslink to the G four positions 5′ of the TAAT sequence (<u>G</u>CGGTAATGAGAT). This crosslink does not map to the same 5′ position as on the octamer site (see Fig. 2 *Lower*) and may result from binding of the POU$_S$ domain in an inverted orientation as seen with Pit-1 (3) and suggested for Brn-2 (5). The relative levels of cleavage 5′ and 3′ of the TAATGARAT sequence are consistent with previous chemical modification interference analyses (6, 14, 15) and mutational analysis (6), which indicate that the POU$_S$ domain is principally positioned over the GARAT element when the Oct-1 POU domain binds to this (OCTA$^-$)TAATGARAT sequence.

The Oct-1 POU Domain Adopts Multiple Conformations on an (OCTA$^+$)TAATGARAT Site. The (OCTA$^+$)TAATGARAT site contains both octamer and (OCTA$^-$)TAATGARAT sequences. Differences in Oct-1 POU domain footprinting patterns of (OCTA$^+$)TAATGARAT sites with wild-type and mutant GARAT sequences have suggested that the Oct-1 POU domain adopts an unusual conformation on the wild-type site (12). We used domain-specific crosslinking to probe this unusual conformation.

Fig. 3 shows the cleavage patterns resulting from crosslinking to both strands of the (OCTA$^+$)TAATGARAT site. The POU$_{H\text{-}UC7}$ protein crosslinked to both strands of this site just upstream of the TAAT sequence (lanes 3 and 6), suggesting that, on this site, the POU$_H$ domain binds uniquely to the TAAT sequence in the same orientation as it binds to the octamer and (OCTA$^-$)TAATGARAT sites. In contrast, the POU$_S$ domain crosslinked to the (OCTA$^+$)TAATGARAT site at several locations both 5′, as on an octamer site, and 3′, as on an (OCTA$^-$)TAATGARAT site, of the TAAT sequence (Fig. 3, lanes 2 and 5, and *Lower*), suggesting that the Oct-1 POU domain adopts at least two very different conformations on this site. In the region 5′ of the TAAT POU$_H$-domain-binding site, the POU$_S$ domain generates two crosslink-induced cleavages on each strand (Fig. 3, lanes 2 and 5, and *Lower*). The TAAT-proximal cleavages probably reflect Oct-1 binding in an octamer-site-like conformation; the other two cleavages may reflect an inverted POU$_S$-domain orientation similar to that described for the Pit-1 POU domain (3).

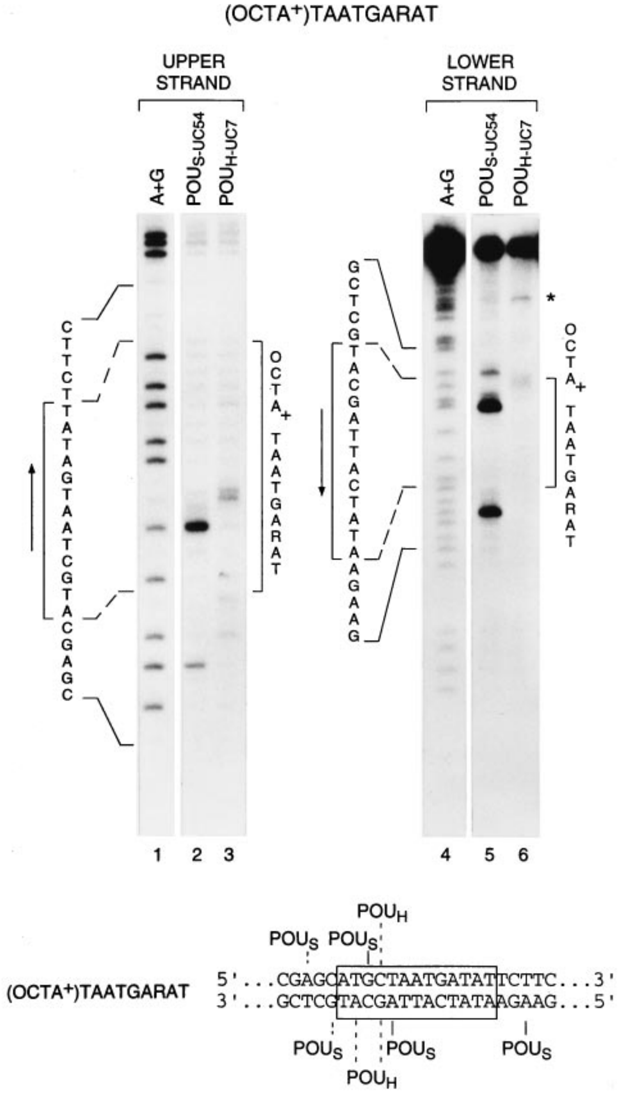

FIG. 3. The POU domain adopts multiple conformations on an (OCTA$^+$)TAATGARAT site. Shown are the cleavage products generated from POU domain–DNA crosslinking to both strands of the (OCTA$^+$)TAATGARAT site. Lanes 2 and 3, cleavage pattern generated on the upper strand. The POU$_H$ doublet may be due to an incomplete cleavage reaction. Lanes 5 and 6, cleavage pattern generated on the lower strand. Lanes 1 and 4 (A+G), purine-cleavage pattern of the strand indicated. In lanes 5 and 6, the uppermost bands represent uncleaved DNA. Brackets, arrows, and asterisk are as in Fig. 2. (*Lower*) Summary of positions of cleavage. Dashed lines indicate lower-yield cleavage products.

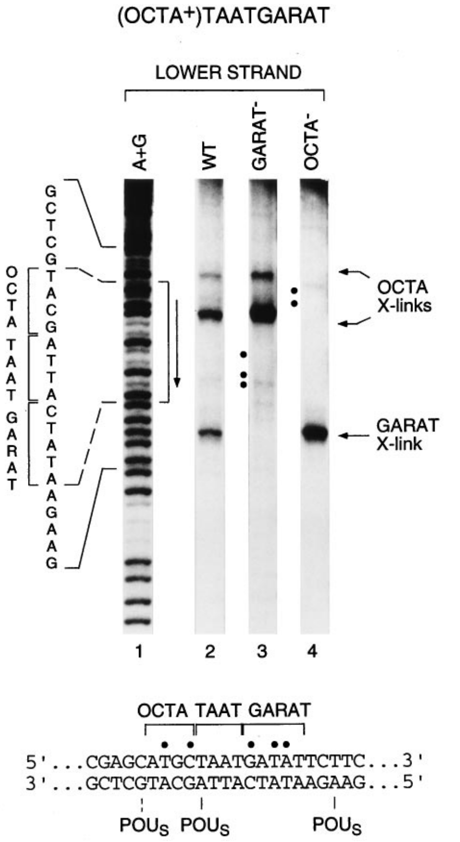

FIG. 4. The POU$_S$ domain binds to the wild-type half-site in mutant forms of the (OCTA$^+$)TAATGARAT site. Shown are the cleavage products generated from crosslinking of the POU$_S$ domain to wild-type (lane 2) and mutant (lanes 3 and 4) (OCTA$^+$)-TAATGARAT sites. Lane 1 (A+G), purine-cleavage pattern of the wild-type probe; lane 3, (OCTA$^+$)TAATGARAT site with the mutated 3′ GARAT sequence (underlined), . . . AT**TAGCT**TC. . . (mutations shown in bold); lane 4, (OCTA$^+$)TAATGARAT site with the mutated 5′ OCTA sequence (underlined), . . . GC**AAGG**TA. . . (mutations shown in bold). Brackets and vertical arrows are as in Fig. 2. (*Lower*) Sequence with sites of mutations marked by dots and crosslinking sites indicated. Dashed line indicates lower-yield cleavage product.

To examine whether the POU$_S$ domain can bind independently either 5′ or 3′ of the POU$_H$ domain-binding site of the (OCTA$^+$)TAATGARAT sequence, we compared crosslinking of the POU$_{S\text{-UC54}}$ protein bound to the wild-type (OCTA$^+$)TAATGARAT sequence with crosslinking to two mutant forms of the site in which either the 5′ or 3′ POU$_S$ domain-binding site has been disrupted. As indicated in Fig. 4 by dots, we mutated residues in the POU$_S$ domain-binding sites but not the precise sites of crosslinking. Consistent with independent binding of the POU$_S$ domain to the 5′ ATGC element and the 3′ GARAT element, when the GARAT region of the (OCTA$^+$)TAATGARAT sequence is mutated, we only detect cleavages in the upstream ATGC portion of the octamer site (compare lane 3 with lane 2). Likewise, when the upstream ATGC portion of the octamer site is mutated, we only detect cleavages near the GARAT sequence (compare lane 4 with lane 2). These results demonstrate that two functionally independent, but overlapping, POU domain-binding sites make up the (OCTA$^+$)TAATGARAT element.

These results may also explain why hydroxy-radical footprinting reveals a POU$_H$-domain TAAT protection pattern but not a POU$_S$-domain protection pattern when the POU domain is bound to an (OCTA$^+$)TAATGARAT site (12). Whereas the POU$_H$ domain apparently binds stably to the TAAT sequence, the POU$_S$ domain can bind either upstream or downstream of the POU$_H$ domain, thus serving as an ineffective inhibitor of hydroxy-radical attack of the sequences flanking the POU$_H$ domain-binding site. Consistent with this hypothesis, when the GARAT sequence is mutated, the Oct-1 POU domain effectively protects the 5′ ATGC element (12). Together, the footprinting (12) and crosslinking (this study) results suggest that the Oct-1 POU domain structure is dynamic on an (OCTA$^+$)TAATGARAT site.

VP16 Associates with Multiple Oct-1 POU-Domain Conformations. The multiple conformations of the Oct-1 POU domain on the (OCTA$^+$)TAATGARAT site raise the issue of how the Oct-1 POU domain is structured in a VP16-induced complex. The structure of the VP16-induced complex is unclear, principally because VP16 binds DNA poorly in the absence of Oct-1 (16, 17). Thus, although the GARAT and neighboring 3′ sequences are specifically important for forming a VP16-induced complex (18–22), it is not known whether these sequences induce an Oct-1 POU-domain conformation compatible with recognition by VP16 (12) or create a VP16-binding site (see ref. 4).

To probe the conformation of the Oct-1 POU domain in a VP16-induced complex, we devised a crosslinking strategy analogous to chemical modification interference analysis. We first crosslinked either the POU$_{\text{S}}$ or POU$_{\text{H}}$ domain to the (OCTA$^+$)TAATGARAT site and then selected those crosslinked species that could still form a complex with VP16 (see *Materials and Methods*). If a particular conformation of the POU domain is incompatible with VP16-induced complex formation, crosslinks resulting from that conformation should interfere with VP16-induced complex formation and be missing in the DNAs selected for VP16-induced complex formation. We refer to this strategy as "crosslinking interference analysis."

Fig. 5 shows the results of the crosslinking interference analysis with POU$_{\text{S}}$- (POU$_{\text{S-UC54}}$; lanes 2–4) and POU$_{\text{H}}$- (POU$_{\text{H-UC50}}$; lanes 5–7) specific crosslinkers. Because the level of POU$_{\text{H-UC7}}$ cleavage on the (OCTA$^+$)TAATGARAT site was not sufficient for the crosslinking interference analysis (see Fig. 3), we used the natural POU$_{\text{H}}$-domain cysteine in POU$_{\text{H-UC50}}$ for this analysis. Cysteine 50 lies in the DNA-recognition helix and contacts the DNA major groove in the octamer cocrystal structure (2); we did not use this crosslinker in the analyses described above to avoid crosslinker-induced changes in POU$_{\text{H}}$-domain binding to the DNA.

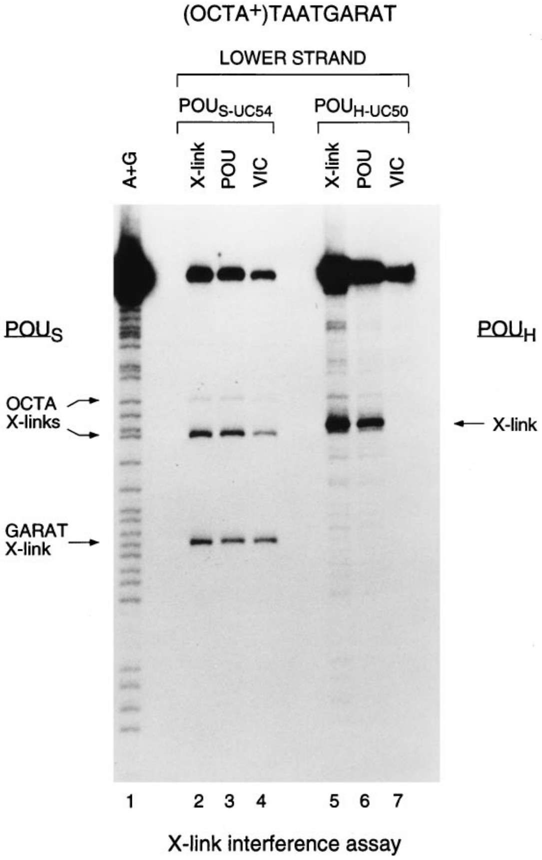

FIG. 5. VP16 associates with multiple conformations of the Oct-1 POU domain. Shown are the results of a crosslinking interference analysis of two unique-cysteine derivatives of the POU domain, POU$_{\text{S-UC54}}$ (lanes 2–4) and POU$_{\text{H-UC50}}$ (lanes 5–7), crosslinked to the lower strand of the (OCTA$^+$)TAATGARAT site. POU$_{\text{S}}$ crosslinks over the 5′ ATGC (OCTA X-links) or 3′ GARAT (GARAT X-link) sequences and POU$_{\text{H}}$ crosslinks (X-link) are indicated. In lanes 2–7, the uppermost bands represent uncleaved DNA. X-link (above lanes), standard crosslinking analysis of the POU domain alone to the site; POU, crosslinking pattern of the POU-domain complex after electrophoretic mobility retardation; VIC, crosslinking interference pattern of the VP16-induced complex after electrophoretic mobility retardation.

Because cysteine 50 is directed 3′ of the octamer sequence (2) in the Oct-1 POU-domain–octamer site crystal structure, we expected POU$_{\text{H-UC50}}$ crosslinking to occur within the GARAT sequence. The observed crosslink-induced cleavage, however, maps 5′ of this region at the G residue in the C:G base pair at the fourth position within the octamer sequence (ATGCTAAT; Fig. 5, lane 5). This difference may reflect an alteration of the precise conformation of the POU$_{\text{H-UC50}}$ domain on DNA induced by (*i*) the different binding sites [H2B octamer vs. (OCTA$^+$)TAATGARAT] or (*ii*) the crosslinking moiety. Whichever the case, the POU$_{\text{H-UC50}}$ crosslink interferes very strongly with VP16-induced complex formation (compare lanes 6 and 7). These results demonstrate that it is possible to interfere with VP16-induced complex formation by crosslinking and suggest that the conformation, precise position, or flexibility of the POU$_{\text{H}}$ domain on the (OCTA$^+$)TAATGARAT site is critical for association of the Oct-1 POU domain with VP16.

In striking contrast to the strong interference caused by the POU$_{\text{H-UC50}}$ crosslink, the POU$_{\text{S-UC54}}$ crosslinks, either at or near the octamer ATGC sequence (OCTA X-links) or near the GARAT sequence (GARAT X-link), are compatible with VP16-induced complex formation (Fig. 5, compare lanes 3 and 4). An apparent slight decrease in crosslink-induced cleavages at the octamer ATGC sequence (compare lanes 3 and 4) may suggest a preference for POU$_{\text{S}}$-domain binding to the GARAT sequence in a VP16-induced complex. Nevertheless, crosslinking of the POU$_{\text{S}}$ domain to the ATGC sequence is compatible with VP16-induced complex formation, demonstrating that VP16 can associate with multiple conformations of the Oct-1 POU domain.

DISCUSSION

We have probed the structure of the Oct-1 POU domain on different cis-regulatory sites and in a multiprotein complex. The structures of DNA-bound POU domains have been previously studied by x-ray crystallography (2, 3) and by mutagenesis (5, 6); crystallography, however, inherently provides only a static view of macromolecular interactions, and mutational analyses are indirect. Here, we have used protein–DNA photocrosslinking in a domain-specific manner to probe directly the conformation of the Oct-1 POU domain on DNA and in the VP16-induced complex. The photocrosslinking method we used (7) was particularly well suited for this analysis because the crosslinker is placed at a unique position on the protein and multiple sites of crosslinking to the DNA can be easily mapped with end-labeled probes. The results of our crosslinking studies of the two DNA-binding domains of the Oct-1 POU domain on different regulatory sites revealed the dynamic nature of Oct-1 binding to a single regulatory site—the (OCTA$^+$)TAATGARAT site—and crosslinking interference revealed flexibility of the Oct-1 POU domain in VP16-induced complex formation.

We used three different Oct-1-binding sites in our studies—the high-affinity histone H2B octamer sequence and two VP16-responsive elements, an (OCTA$^-$) and (OCTA$^+$) TAATGARAT site—and each has revealed different arrangements of the Oct-1 POU domain as illustrated in Fig. 6. The pattern of crosslinking to the octamer site agrees with that predicted by the crystal structure (2), suggesting that, in solution, the POU-domain structure adopts the unique conformation elucidated crystallographically. Crosslinking to the (OCTA$^-$)TAATGARAT site provides physical evidence for the unexpected structure of the Oct-1 POU domain revealed on this site by mutational analysis (6), with the POU$_{\text{S}}$ domain principally positioned over the GARAT element and thus to

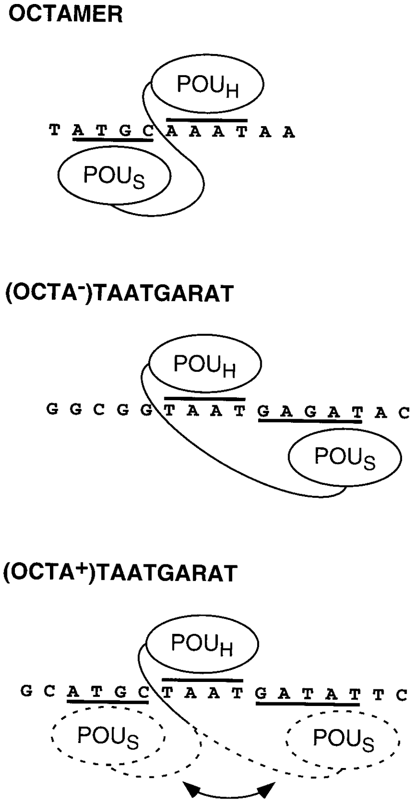
OCTAMER

(OCTA^{-})TAATGARAT

(OCTA^{+})TAATGARAT

FIG. 6. Model for binding of the Oct-1 POU domain to three DNA targets, the octamer and the (OCTA^{-}) and (OCTA^{+}) TAATGARAT sites, highlighting conformational flexibility in Oct-1 POU DNA-binding domain arrangement.

the opposite side of the POU$_{\text{H}}$ domain than when bound to the octamer sequence. The results of crosslinking to the (OCTA^{+})TAATGARAT site show that the Oct-1 POU domain can adopt either the octamer-like or (OCTA^{-})-TAATGARAT-like conformation on the single binding site. These results lead to the view of a dynamic Oct-1 POU domain on an (OCTA^{+})TAATGARAT site: while the POU$_{\text{H}}$ domain remains fixed, the POU$_{\text{S}}$ domain swings from one POU$_{\text{S}}$-domain-binding site to the next.

The role of the Oct-1 POU$_{\text{S}}$ domain in VP16-induced complex formation—beyond its requirement for effective DNA binding by the Oct-1 POU domain (23)—is unclear, as is its position in the complex. It is known that the POU$_{\text{S}}$ domain is not essential for VP16-induced complex formation (16, 24); indeed, the POU$_{\text{S}}$ domain can be replaced by a completely different DNA-binding module, and the resulting chimeric "POU domain" can support efficient VP16-induced complex formation (25). In the native POU domain, however, the POU$_{\text{S}}$ domain may play a specific role, because mutations in the POU$_{\text{S}}$ domain can have a selective effect on VP16-induced complex formation on an (OCTA^{-})TAATGARAT site (6).

The crosslinking interference analysis described here with an (OCTA^{+})TAATGARAT site shows that, whether the POU$_{\text{S}}$ domain lies over the OCTA element 5′ of the POU$_{\text{H}}$ domain or the GARAT element 3′ of the POU$_{\text{H}}$ domain, the Oct-1 POU domain can associate with VP16. Consistent with these results even in a natural (OCTA^{+})TAATGARAT VP16-induced complex, the POU$_{\text{S}}$ domain can be crosslinked by UV irradiation to either the OCTA or GARAT sequences (unpublished results).

These results impact on our view of the VP16-induced complex. First, because the POU$_{\text{S}}$ domain need not be bound to the GARAT element to promote VP16-induced complex formation, the essential function of the GARAT element in VP16-induced complex formation (18–20) is probably not to provide a binding site for the Oct-1 POU$_{\text{S}}$ domain. Instead, it is more likely that the GARAT element is essential for VP16-induced complex formation because it provides an essential binding site for VP16. Second, the ability of the POU$_{\text{S}}$ domain to promote VP16-induced complex formation when crosslinked to the GARAT element suggests that VP16 and the POU$_{\text{S}}$ domain can co-occupy the GARAT element. We do not know how such co-occupancy may occur. The simple hypothesis that VP16 and the Oct-1 POU$_{\text{S}}$ domain bind to different faces of the DNA is probably not correct, because analysis of VP16-induced complex formation with inosine-substituted DNA probes suggests that VP16 and the Oct-1 POU$_{\text{S}}$ domain both recognize sequence determinants in the major groove of the DNA (13).

In conclusion, these studies reveal an extraordinary level of structural versatility and adaptability in how two macromolecules—a protein and DNA—interact with each other. As the DNA changes structure, as in the different sequences of the cis-regulatory sites, the protein—the Oct-1 POU domain—responds by also changing its structure.

We thank N. Hernandez, L. Joshua-Tor, B. Stillman, and W. Tansey for critical readings of the manuscript, and J. Duffy and P. Renna for artwork. P.S.P. thanks N. Hernandez for support and encouragement. These studies were supported by Public Health Service Grant CA13106 from the National Cancer Institute.

1. Herr, W., Sturm, R. A., Clerc, R. G., Corcoran, L. M., Baltimore, D., Sharp, P. A., Ingraham, H. A., Rosenfeld, M. G., Finney, M., Ruvkun, G. & Horvitz, H. R. (1988) *Genes Dev.* **2,** 1513–1516.
2. Klemm, J. D., Rould, M. A., Aurora, R., Herr, W. & Pabo, C. O. (1994) *Cell* **77,** 21–32.
3. Jacobson, E. M., Li, P., Leon-del-Rio, A., Rosenfeld, M. G. & Aggarwal, A. K. (1997) *Genes Dev.* **11,** 198–212.
4. Herr, W. & Cleary, M. A. (1995) *Genes Dev.* **9,** 1679–1693.
5. Li, P., He, X., Gerrero, M. R., Mok, M., Aggarwal, A. & Rosenfeld, M. G. (1993) *Genes Dev.* **7,** 2483–2496.
6. Cleary, M. A. & Herr, W. (1995) *Mol. Cell. Biol.* **15,** 2090–2100.
7. Pendergrast, P. S., Chan, Y., Ebright, Y. W. & Ebright, R. H. (1992) *Proc. Natl. Acad. Sci. USA* **89,** 10287–10291.
8. Lai, J.-S., Cleary, M. A. & Herr, W. (1992) *Genes Dev.* **6,** 2058–2065.
9. Maxam, A. M. & Gilbert, W. (1980) *Methods Enzymol.* **65,** 499–560.
10. Wilson, A. C., LaMarco, K., Peterson, M. G. & Herr, W. (1993) *Cell* **74,** 115–125.
11. apRhys, C. M. J., Ciufo, D. M., O'Neill, E. A., Kelly, T. J. & Hayward, G. S. (1989) *J. Virol.* **63,** 2798–2812.
12. Walker, S., Hayes, S. & O'Hare, P. (1994) *Cell* **79,** 841–852.
13. Cleary, M. A. (1995) Ph.D. thesis (Univ. of New York, Stony Brook).
14. Baumruker, T., Sturm, R. & Herr, W. (1988) *Genes Dev.* **2,** 1400–1413.
15. Preston, C. M., Frame, M. C. & Campbell, M. E. M. (1988) *Cell* **52,** 425–434.
16. Kristie, T. M. & Sharp, P. A. (1990) *Genes Dev.* **4,** 2383–2396.
17. Stern, S. & Herr, W. (1991) *Genes Dev.* **5,** 2555–2566.
18. Gerster, T. & Roeder, R. G. (1988) *Proc. Natl. Acad. Sci. USA* **85,** 6347–6351.
19. O'Hare, P. O., Goding, C. R. & Haigh, A. (1988) *EMBO J.* **7,** 4231–4238.
20. Kristie, T. M., LeBowitz, J. H. & Sharp, P. A. (1989) *EMBO J.* **8,** 4229–4238.
21. Huang, C. C. & Herr, W. (1996) *Mol. Cell. Biol.* **16,** 2967–2976.
22. Misra, V., Walter, S., Yang, P., Hayes, S. & O'Hare, P. (1996) *Mol. Cell. Biol.* **16,** 4404–4413.
23. Sturm, R. A. & Herr, W. (1988) *Nature (London)* **336,** 601–604.
24. Katan, M., Haigh, A., Verrijzer, C. P., van der Vliet, P. C. & O'Hare, P. (1990) *Nucleic Acids Res.* **18,** 6871–6880.
25. Pomerantz, J. L., Pabo, C. O. & Sharp, P. A. (1995) *Proc. Natl. Acad. Sci USA* **92,** 9752–9756.